DSTO

The Yield Behaviour of a Structural Adhesive under Complex Loading

Mladen Ignjatovic, Peter Chalkley and Chung Wang

DSTO-TR-0728

DEPARTMENT OF DEFENCE

DEFENCE SCIENCE AND TECHNOLOGY ORGANISATION

The Yield Behaviour of a Structural Adhesive under Complex Loading

Mladen Ignjatovic, Peter Chalkley and Chun Wang

Airframes and Engines Division
Aeronautical and Maritime Research Laboratory

DSTO-TR-0728

ABSTRACT

Recent developments in bonded composite repair technology at the Aeronautical and Maritime Research Laboratory (AMRL) have been in the area of repairs to curved surfaces, eg. the proposed repairs to the F/A-18 aileron hinge and the F/A-18 bulkhead crotch region. Bonded composite repairs to curved surfaces induce through-thickness stresses as well as shear stresses in the adhesive. The yield behaviour of AMRLs most common repair adhesive - FM73 - has not been investigated under such conditions of combined loading.

Reported herein is a yield function for the repair adhesive FM73, based upon the Modified Drucker-Prager/Cap Plasticity model. This yield function was selected based on experiments on a test specimen subjected to a range of combined stress states. A finite element (FE) analysis of test specimen (Iosipescu test specimen modified for adhesives) was carried out to establish its validity for obtaining data.

A set of constants was obtained for the Modified Drucker-Prager/Cap Plasticity model of FM73 adhesive that enables detailed FE analyses of bonded repairs to curved surfaces.

RELEASE LIMITATION

Approved for public release

DEPARTMENT OF DEFENCE

DEFENCE SCIENCE AND TECHNOLOGY ORGANISATION

Published by

DSTO Aeronautical and Maritime Research Laboratory
PO Box 4331
Melbourne Victoria 3001 Australia

Telephone: (03) 9626 7000
Fax: (03) 9626 7999

AR-010-646
September 1998

APPROVED FOR PUBLIC RELEASE

The Yield Behaviour of a Structural Adhesive under Complex Loading

Executive Summary

Bonded composite repair technology has been used with great success over the past twenty-five years to repair and reinforce damaged structure in Royal Australian Air Force (RAAF) aircraft. These repairs have been primarily applied to flat and/or lightly loaded structures. Recent developments in the bonded composite repair technology at the Aeronautical and Maritime Research Laboratory (AMRL) have been in the area of repairs to highly-loaded curved surfaces, eg. the proposed repairs to the RAAFs F/A-18 aileron hinges and F/A-18 bulkhead crotch regions. Repairs to curved surfaces introduce a new challenge because the adhesive is subjected to a complex stress state unlike in flat surface repairs in which the stress state is predominantly one of simple shear. A yield criterion that can accommodate complex stress states in the adhesive is needed if reliable stress analyses of repairs to curved surfaces are to be achieved. The yield behaviour of the AMRLs most common repair adhesive - FM73 - has not been investigated under such conditions.

This report investigates a yield function for the repair adhesive FM73 subjected to complex stress states. Various yield criteria were compared with the results of a series of experments. Based on experimental results, it was found that the Modified Drucker-Prager/Cap Plasticity model offers the best correlation with the observed behaviour. The results of this work enable detailed stress analysis of repairs to curved surfaces to be carried out using finite element methods.

Authors

Mladen Ignjatovic
Airframes and Engines Division

Mladen undertook this work as part of his vocation training whilst completing an Aerospace Engineering Degree at the Royal Melbourne Institute of Technology.

Peter Chalkley
Airframes and Engines Division

Peter Chalkley is a Professional Officer at AMRL and has a B.Sc. (Hons) in Metallurgy from the UNSW and a M.Sc. in Mathematics from the University of Melbourne and is curently a member of the Australian Composites Structures Society. He joined AMRL in 1986 and has worked on the materials science of adhesives and composite materials.

Chun Wang
Airframes and Engines Division

Chun-Hui Wang has a B.Eng and Ph.D (Sheffield, UK) in Mechanical Engineering and is currently a member of the Institute of Engineers, Australia. Prior to joining the Aeronautical and Maritime Research Laboratory in 1995 as a Senior Research Scientist, Dr. Wang was a Lecturer at the Deakin University. He has an extensive research record in fatigue and fracture mechanics, stress analysis and constitutive modelling, and biomechanics. Over the last six years he also held academic/research positions at the University of Sydney and the University of Sheffield, UK.

Contents

1. INTRODUCTION 1

2. CANDIDATE ADHESIVE YIELD CRITERIA 1
2.1 Maximum-Shear-Stress (Tresca) Yield Criterion 2
1.2 Distortion-Energy (von Mises) Yield Criterion 4
1.3 Mohr-Coulomb Yield Criterion 5
1.4 Modified Tresca Yield criterion 5
1.5 Modified von Mises Yield Criterion 6
1.6 Drucker-Prager Plasticity Model 6
2.7 Modified Drucker-Prager/Cap Plasticity Model 7

3. FM73 ADHESIVE TESTING 8
3.1 Modified Iosipescu Test Specimen 9
3.2 The Modified Iosipescu Test Rig 9
3.3 Determination of the Yield Stress for Combined Stress States 11
3.4 Shear, Shear-Tension and Shear-Compression Results 11
3.5 Uniaxial Tension/Compression Test Results 12
3.6 Failure Modes 13

4. EVALUATION OF YIELD CRITERIA 15
4.1 von Mises & Tresca Criteria 15
4.2 Modified von Mises and Modified Tresca Criteria 16
4.3 Drucker-Prager and Modified Drucker-Prager/Cap Plasticity Model. 18

5. FINITE ELEMENT MODELLING 19
5.1 Procedure 19
5.2 Results 21

6. CONCLUSIONS 25

7. REFERENCES 26

APPENDICES 27

APPENDIX 1 - STATE OF STRESS IN THREE DIMENSIONS 27

APPENDIX 2 - FORCE-DISPLACEMENT GRAPHS 29

1. Introduction

Adhesively bonded joints have been widely employed in the aerospace industry for the joining, reinforcement and repair of components. The critical role of the adhesive is to transfer load from one adherend to another. In bonded composite repairs, particularly to thick-section primary aircraft structure, the adhesive is often highly loaded and prone to yielding under in-service loads. A further complication arises in the context of repairs applied to curved surfaces in which a combination of normal and shear stresses is present. Consequently, an experimentally validated adhesive yield criterion that can account for combined stress states is essential for accurate stress analyses of such bonded repairs.

Two applications to curved surfaces that are currently being investigated at AMRL are the repair of aileron hinge and the 470.5 bulkhead crotch region on the RAAF's F/A-18's [1]. In these repairs, through-thickness tensile stresses as well as shear stresses are present in the adhesive layer. The stress mix in the adhesive of these repairs varies from pure shear in some regions to shear/tension to shear/compression to pure tension in other areas. These repairs differ from many of AMRL's earlier repairs [2] in which the adhesive was predominantly in a state of shear, for which the yield behaviour was well established.

The yield behaviour of polymers, such as adhesives, is known to be influenced by the hydrostatic pressure [3]. Yield criteria such as Von-Mises and Tresca can be modified to include a term that accounts for hydrostatic stresses (pressure) and adequately model the behaviour of many adhesives. The adhesive under consideration here is that used in most of AMRL's bonded repairs - the structural epoxy FM73 (manufactured by Cytec). Little data is available, however, for structural adhesives used in bonded repair, including FM73. This report sets out to address this through testing various candidate criteria against experimental data acquired over a range of stress states. The specimen used to evaluate yield behaviour in the presence of combined states is the modified Iosipescu specimen [4,5].

The plan of the report is as follows: in Section 2 the various candidate yield criteria that are commonly employed are reviewed; in Section 3 the test technique and results are described; in Section 4 the candidate yield criteria are evaluated against the experimental data and the best criterion chosen and in Section 5 the finite-element analyses of various specimen configurations to validate the test technique are described.

2. Candidate Adhesive Yield Criteria

Several yield criteria were chosen as the candidate adhesive yield criteria for analysis and development of the FM73 adhesive yield function. Maximum-Shear-Stress [6] and

Distortion-Energy [6] yield criteria, better known as Tresca and von Mises, which were developed as the yield functions of ductile metals, were chosen for analysis because they are implemented in the finite element code ABAQUS which is renowned for its advanced capabilities in non-linear analysis. Mohr-Coulomb [3,7] as well as the modified Tresca [3,7] and modified von Mises [3,7] yield criteria were considered as they are often suggested for adhesive yield function studies. Drucker-Prager [8,9,10] and modified Drucker-Prager/Cap Plasticity [8,9,10] yield criteria were also investigated as they are implemented by ABAQUS for non-linear analysis of porous materials.

Since the adherends used in the investigation have much higher moduli of elasticity than the adhesive, the adhesive was considered to be highly constrained. This leads to the assumption of plane strain conditions in the adhesive layer in the bonded joint. The candidate yield criteria have been therefore modified to account for this assumption.

2.1 Maximum-Shear-Stress (Tresca) Yield Criterion

The Tresca Yield criterion [6] is a mathematically simple criterion, based on the assumption that plastic yielding occurs when the maximum shear stress, τ_{max}, exceeds the maximum shear stress measured under uniaxial tension, τ_0. Mathematically, the maximum shear stress is expressed as

$$\tau_{\max} = \frac{\sigma_1 - \sigma_3}{2} \tag{2.1}$$

where σ_1 and σ_3 are respectively the maximum and minimum principal stresses.

According to the Tresca Yield criterion, yielding occurs when $\tau_{\max} = \tau_0$. In the case of uniaxial tension, $\sigma_1 = \sigma_0$, $\sigma_2 = \sigma_3 = 0$ and $\tau_0 = \frac{\sigma_0}{2}$.

Therefore,

$$\sigma_1 - \sigma_3 = \sigma_0. \tag{2.2}$$

For pure shear $\sigma_1 = -\sigma_3 = 2k = \sigma_o$ and $\sigma_2 = 0$, so that:

$$k = \frac{\sigma_0}{2}. \tag{2.3}$$

Although it is mathematically simple, the disadvantage of this criterion is that it requires the maximum and minimum principal stresses to be known.

The criterion can be simplified for plane strain conditions (see Appendix 1) and may be written as

$$\sigma_{1,3} = \frac{(\sigma_x + \sigma_y) \pm \sqrt{(\sigma_x + \sigma_y)^2 - 4(\sigma_x \sigma_y - \tau_{xy}^2)}}{2} \tag{2.4}$$

and

$$\sigma_2 = \sigma_z = \nu(\sigma_x + \sigma_y) \tag{2.5}$$

where ν is Poisson's ratio.

Substituting Equation (2.4) into maximum shear stress Equation (2.2) gives a more useful form of Tresca Yield criterion

$$\left(\frac{\sigma_x - \sigma_y}{\sigma_0}\right)^2 + 4\left(\frac{\tau_{xy}}{\sigma_0}\right)^2 = 1 \tag{2.6}$$

Furthermore, if highly constrained conditions are assumed, ie. $\varepsilon_y = 0$ as well as $\varepsilon_z = \tau_{yz} = \tau_{xz} = 0$:

$$\varepsilon_y = \frac{1}{E}\left[\sigma_y - \nu(\sigma_z + \sigma_x)\right] = 0 \tag{2.7}$$

$$\varepsilon_z = \frac{1}{E}\left[\sigma_z - \nu(\sigma_x + \sigma_y)\right] = 0 \tag{2.8}$$

hence,

$$\sigma_y = \sigma_z = \sigma_x\left(\frac{\nu + \nu^2}{1 - \nu^2}\right) = \sigma_x\left(\frac{\nu}{1 - \nu}\right). \tag{2.9}$$

Equation 2.6 then becomes:

$$\left(\frac{1 - 2\nu}{1 - \nu}\right)^2\left(\frac{\sigma_x}{\sigma_0}\right)^2 + 4\left(\frac{\tau_{xy}}{\sigma_0}\right)^2 = 1 \tag{2.10}$$

These assumptions regarding the highly constrained nature of the adhesive are verified later in the section on FE analysis.

Although Tresca criterion is known to apply to ductile metals, its validity in case of structural adhesives is often questioned [3], as it does not account for the effect of normal stresses.

2.2 Distortion-Energy (von Mises) Yield Criterion

The von Mises Yield criterion [6], also developed for ductile metals, assumes that plastic yielding occurs when the second invariant, J_2, of the stress deviator exceeds a constant value, k^2, which is related to the yielding stress in uniaxial tension:

$$J_2 = k^2 \tag{2.11}$$

where

$$J_2 = \frac{1}{6}\left[(\sigma_1 - \sigma_2)^2 + (\sigma_2 - \sigma_3)^2 + (\sigma_3 - \sigma_1)^2\right]. \tag{2.12}$$

In uniaxial tension, $\sigma_1 = \sigma_0$ and $\sigma_2 = \sigma_3 = 0$:

$$k = \frac{\sigma_0}{\sqrt{3}}. \tag{2.13}$$

von Mises Yield Criterion is therefore given by:

$$\sigma_0 = \frac{1}{\sqrt{2}}\left[(\sigma_1 - \sigma_2)^2 + (\sigma_2 - \sigma_3)^2 + (\sigma_3 - \sigma_1)^2\right]^{1/2} \tag{2.14}$$

or

$$\sigma_0 = \frac{1}{\sqrt{2}}\left[(\sigma_x - \sigma_y)^2 + (\sigma_y - \sigma_z)^2 + (\sigma_z - \sigma_x)^2 + 6(\tau_{xy}^2 + \tau_{yz}^2 + \tau_{xz}^2)\right]^{1/2}. \tag{2.15}$$

The advantage of the von Mises criterion over the Tresca criterion is that the maximum and minimum principal stresses do not need to be calculated.

From the plane strain conditions $\tau_{xz} = \tau_{yz} = 0$ and $\sigma_z = \nu(\sigma_x + \sigma_y)$. Substituting this condition in Equation (2.11) and rearranging gives a more useful form of von Mises criterion:

$$\left(\frac{\sigma_x - \sigma_y}{\sigma_0}\right)^2 - \nu(1-\nu)\left(\frac{\sigma_x + \sigma_y}{\sigma_0}\right)^2 + 3\left(\frac{\tau_{xy}}{\sigma_0}\right)^2 = 1 \tag{2.16}$$

Under highly constrained conditions this becomes:

$$\left(\frac{1-2\nu}{1-\nu}\right)^2\left(\frac{\sigma_x}{\sigma_0}\right)^2 + 3\left(\frac{\tau_{xy}}{\sigma_0}\right)^2 = 1. \tag{2.17}$$

When investigating the yield behaviour of metals, the von Mises criterion is used more often than the Tresca criterion, because it is found to offer a better agreement with experimental result and it is also mathematically easier to implement.

2.3 Mohr-Coulomb Yield Criterion

The Mohr-Coulomb Yield criterion [3] determines the yield function of soils (eg. building-stone in compression). Yielding is said to occur when the following combination of the shear stress and the normal stress acting on the shear plane attains a critical value, as described by the following equation:

$$\tau_c = \tau_c^{\,0} - \mu_c \sigma_n \tag{2.18}$$

where τ_c^0 and μ_c are cohesion and internal friction coefficient respectively. The advantage of Mohr-Coulomb criterion is that it predicts the angle of the plane, β, on which failure occurs. This angle is proportional to the coefficient of internal friction through the following relationship:

$$-\cot(2\beta) = \mu_c . \tag{2.19}$$

For example, the failure stress of soils has been found to be pressure dependent because the hydrostatic pressure affects the state of the material which in turn has an effect on the yield stress properties. The yield plane is therefore material state and pressure dependent.

Since it was found that the Mohr-Coulomb Yield criterion [3] is not applicable to polymers, both Tresca and von Mises yield criteria have been modified to take into account the pressure sensitivities.

2.4 Modified Tresca Yield criterion

The modified Tresca criterion [3,7] states that the critical shear stress is linearly dependent on the hydrostatic component of the stress tensor, p. The new, pressure-dependent Tresca criterion is given by:

$$\tau_T = \tau_T^{\,0} + \mu_T p \tag{2.20}$$

where

$$p = -\frac{1}{3}(\sigma_1 + \sigma_2 + \sigma_3) \tag{2.21}$$

$$\tau_T = \frac{1}{2}(\sigma_1 - \sigma_3), \tag{2.22}$$

$\tau_T{}^0$ is the yield stress in pure shear, and μ_T denotes the pressure sensitivity of the adhesive.

As the material state varies due to its pressure dependency, μ_T in this case does not define a yield plane but a series of yield surfaces called the yield envelope. For constant values of μ_T, the yield envelope takes the shape of a hexagonal pyramid.

The modified Tresca criterion does not encounter the same problems as the Mohr-Coulomb criterion and is therefore more suited for determining the yield function of polymeric materials.

2.5 Modified von Mises Yield Criterion

The von Mises Yield criterion [3,7] was modified in a similar way to the Tresca Yield criterion in order to account for the hydrostatic component of the stress tensor.

$$\tau_M = \tau_M{}^0 + \mu_M p \tag{2.23}$$

where τ_M in this case is obtained from equation:

$$(\sigma_1 - \sigma_2)^2 + (\sigma_2 - \sigma_3)^2 + (\sigma_3 - \sigma_1)^2 = 6\tau_M{}^2 \tag{2.24}$$

and $\tau_M{}^0$ is the yield stress in pure shear, while p is the hydrostatic component of the stress tensor.

As for the Tresca criterion, μ_M represents a yield envelope in the shape of a right circular cone, but only for constant μ_M values. An advantage over the Tresca criterion is that the von Mises yield surface/envelope (right circular cone) does not encounter the discontinuities present on the Tresca yield surface/envelope (hexagonal pyramid).

2.6 Drucker-Prager Plasticity Model

The finite element code ABAQUS implements Drucker-Prager Plasticity model [8,9,10] as one of the options for simulating yield of porous materials. The expression for the Drucker-Prager failure surface is:

$$F_s = \frac{q}{2}\left[1 + \frac{1}{K} - \left(1 - \frac{1}{K}\right)\left(\frac{r}{q}\right)^3\right] + \frac{1}{3}(\sigma_1 + \sigma_2 + \sigma_3)\tan(\beta) - \left[1 - \frac{1}{3}\tan(\beta)\right]\sigma_c{}^0 = 0, \tag{2.25}$$

or more conveniently:

$$F_s = t - p\tan(\beta) - d = 0, \tag{2.26}$$

where

$$t = \frac{q}{2}\left[1 + \frac{1}{K} - \left(1 - \frac{1}{K}\right)\left(\frac{r}{q}\right)^3\right] \tag{2.27}$$

$$q = \sqrt{3J_2} \tag{2.28}$$

$$r^3 \equiv \frac{27}{2}J_3 = \frac{(2\sigma_1 + \sigma_2 + \sigma_3)(2\sigma_2 + \sigma_3 + \sigma_1)(2\sigma_3 + \sigma_1 + \sigma_2)}{2} \tag{2.29}$$

$$p = -\frac{1}{3}(\sigma_1 + \sigma_2 + \sigma_3) \tag{2.30}$$

$$d = \left[1 - \frac{1}{3}\tan(\beta)\right]\sigma_c^{\,0}. \tag{2.31}$$

Here q is the von Mises equivalent stress and r is the third invariant of the deviatoric stress. The constant β is the material angle of friction. In ABAQUS, its value is given in degrees. σ_c^0 is known as the yield stress in a uniaxial compression, t is the deviatoric stress measure, p is the equivalent pressure stress and d is the material cohesion stress, a material parameter which may depend on some pre-defined fields (eg. temperature). The constant K is defined as the ratio of the flow stress in triaxial tension to the flow stress in triaxial compression and is also a material parameter. The range of K values which provides flexibility when fitting experimental results, is limited in order to ensure convexity of the yield surface:

$$0.778 \le K \le 1.000. \tag{2.32}$$

2.7 Modified Drucker-Prager/Cap Plasticity Model

This model [8,9,10] is an extension of the Drucker-Prager model and was developed for determining the pressure dependent yield failure of cohesive geological materials. There are two parts to the extended model that describe the yield surface of the material. The first part uses the Drucker-Prager model to describe yield surface due to predominantly shearing behaviour and the second is based on a 'cap' which models the hydrostatic pressure effects on the yield surface. The expression for the cap yield surface is given as:

$$F_c = \sqrt{(p - p_a)^2 + \left[\frac{Rt}{1 + \alpha - \alpha / \cos(\beta)}\right]^2} - R\left[d + p_a \tan(\beta)\right] = 0, \quad (2.33)$$

where parameter p_a, known as the evolution parameter, represents the hardening and softening effect created by the volumetric plastic strain:

$$p_a = \frac{p_b - Rd}{1 + R\tan(\beta)}. \quad (2.34)$$

It is partly dependent on the hydrostatic compression yield stress, p_b, which defines the intersection of the equivalent pressure stress axis. Material parameter R is the cap eccentricity and controls the shape of the cap yield surface. It must be greater than 0 and is generally less than 1.0.

$$0 < R < 1.0 \quad (2.35)$$

The parameter α in equation (2.28) is known as the transition surface radius parameter. Its magnitude should be much lower than 1.0 and generally ranges between 0.01 and 0.05. For the material models that include creep properties, α must be 0. In such cases, a transition surface does not exist. Transition surface is another, less important segment of the yield surface region. It was developed in order to create a smooth transition between the shear failure surface and the cap surface, but is not significant in the initial stages of yield function fitting to the experimental results.

3. FM73 Adhesive Testing

The structural adhesive considered in this report is FM73 from Cytec. It is a high strength, rubber modified, structural epoxy that comes in the form of a film on a roll. The manufacturer's suggested cure cycle is 1 hour at 120°C at 300 kPa. The adhesive has a woven polyester carrier cloth. The diamond shaped carrier cloth can be seen in Figures 3.3 to 3.6. The weight of the adhesive film is 0.085 g/sq.m. adhesive film was put through a B-stage (30 minutes at 80°C) before assembly of the specimen for bonding in order to drive off volatiles.

The adhesive yield behaviour was studied over stress states ranging from pure tension to tension/shear to pure shear to shear/compression to pure compression. Tests in the tension/shear and shear/compression range were applied using the modified Iosipescu specimen [4,5]. The Iosipescu test specimen was originally designed for use with fibre-composite materials but has been adapted by Broughton [4,5] and others for use with adhesives. Neat adhesive specimen tests were conducted to obtain the tension

and compression results. The constrained tension results were obtained from a butt joint test.

3.1 Modified Iosipescu Test Specimen

The design of the modified Iosipescu test specimen is shown below (Figure 3.1). The adherends were made of aluminium alloy 2024-T3. The bonding surfaces of the two adherends were prepared by solvent cleaning, grit blasting then an organosilane treatment process. Bonding was carried out in a bonding jig to ensure alignment of the specimen halves.

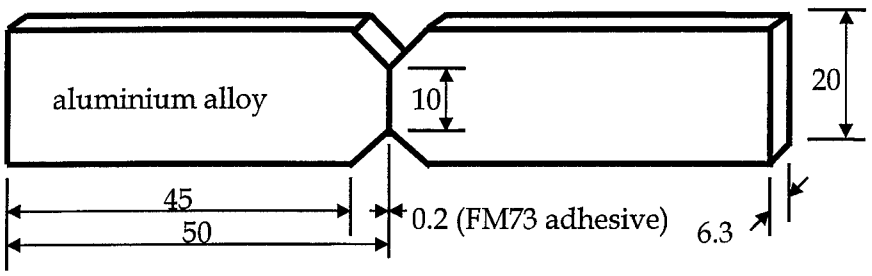

Figure 3.1. Iosipescu test specimen (All dimensions are in millimetres.)

3.2 The Modified Iosipescu Test Rig

The modified Iosipescu test rig, as originally used by Broughton, is shown in Figure 3.2. The rig allows a compressive load P_α, to be applied at an angle α to the longitudinal axis of the bondline (see Fig 3.3). A biaxial stress state subsequently develops in the adhesive bondline with the stresses given by:

$$\sigma_x = \frac{-P_\alpha \sin(\alpha)}{A} \tag{3.1}$$

$$\tau_{xy} = \frac{-P_\alpha \cos(\alpha)}{A} \tag{3.2}$$

where A is the bondline area, σ_x is the through-thickness tensile stress and τ_{xy} the shear stress.

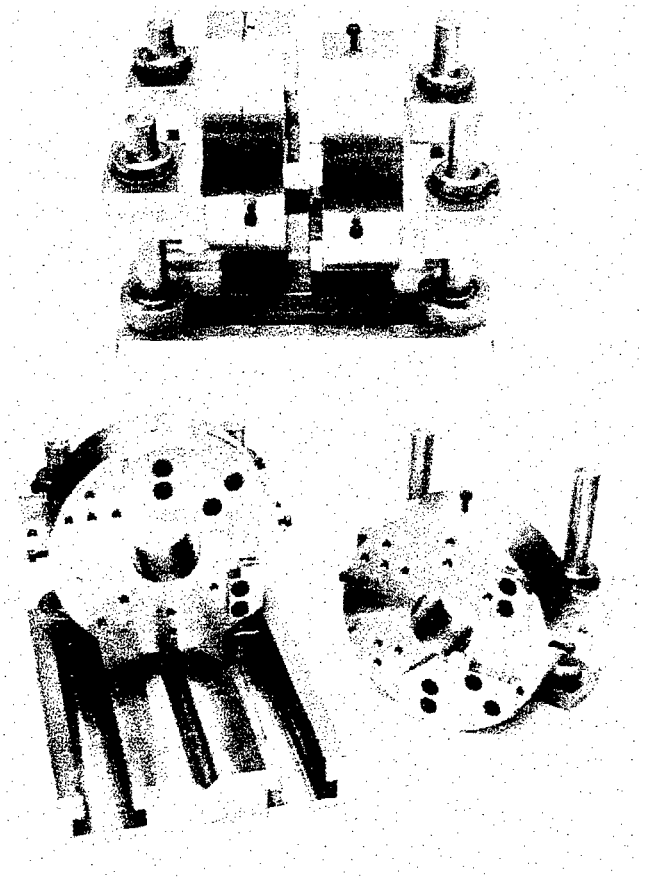

Figure 3.2. The modified Iosipescu test rig.

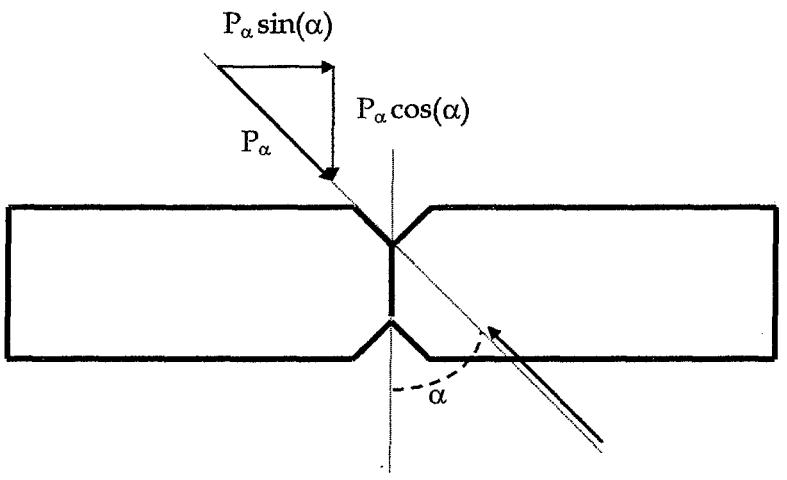

Figure 3.3. Iosipescu test specimen under combined loading.

3.3 Determination of the Yield Stress for Combined Stress States

A typical force-displacement curve obtained from specimen testing is shown in Fig 3.4. The yield load was found by taking the tangents to elastic and plastic regions on the force-displacement graphs, taking the bisector of those tangents, and finding the intersection point with the measured curve. The initial part of the load-displacement curve, where some slop in the loading mechanism is being taken up, is neglected. The yield loads obtained for all stress states are listed in Tables 3.1, 3.2 and 3.3.

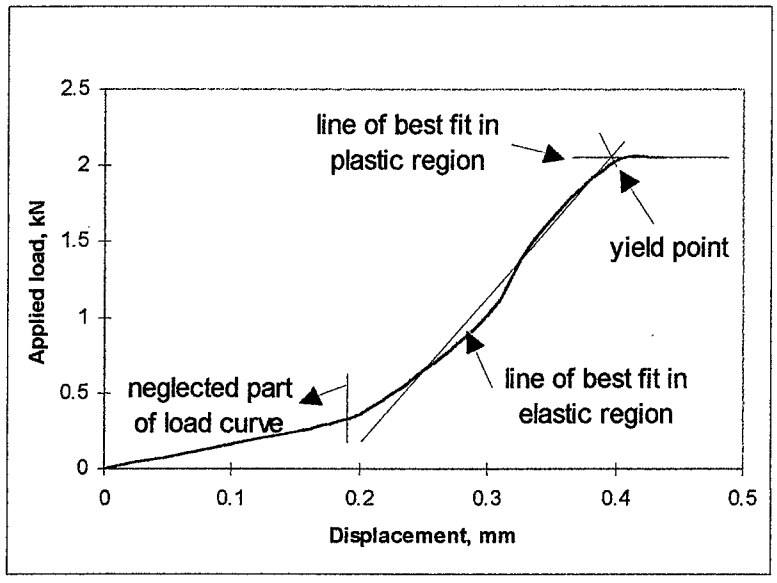

Figure 3.4. Determination of the yield load from load-displacement curves.

3.4 Shear, Shear-Tension and Shear-Compression Results

The following yield stress results were obtained on FM73 adhesive from Iosipescu specimen testing using the modified Iosipescu test rig. Stresses σ_y and σ_x were calculated using Equation

Table 3.1. Yield stress of FM73 adhesive in shear and combined shear-tension and shear-compression.

	Spec.	Adhesive thick. (mm)	Yield load (kN)	Load angle (deg)	Stresses (MPa)			
					σ_x	σ_y	σ_z	τ_{xy}
Pure shear	Al #2	0.12	2.35	0.00	0.00	0.00	0.00	37.30
	Al #1	0.18	2.03	0.00	0.00	0.00	0.00	32.14
	Al #3	0.20	2.15	0.00	0.00	0.00	0.00	34.13
Shear-tension	Al #10	0.22	2.20	-17.19	10.32	5.56	5.56	33.36
	Al #11	0.24	2.15	-17.19	10.09	5.43	5.43	32.60
	Al #4	0.14	2.15	-33.23	18.70	10.07	10.07	28.55
	Al #5	0.16	2.00	-33.23	17.40	9.37	9.37	26.55
Shear-comp.	Al #13	0.12	2.50	17.19	-11.73	-6.31	-6.31	37.91
	Al #12	0.14	2.60	17.19	-12.20	-6.57	-6.57	39.43
	Al #18	0.16	2.55	22.92	-15.76	-8.49	-8.49	37.28
	Al #19	0.22	2.65	28.65	-20.17	-10.86	-10.86	36.91

3.5 Uniaxial Tension/Compression Test Results

For the constrained uniaxial tension test, the modified Iosipescu test specimen was loaded in tension (essentially a butt joint). The following results were obtained:

Table 3.2 Yield stress of FM73 adhesive in constrained uniaxial tension.

	Spec.	Adhesive thick. (mm)	Yield load (kN)	Load angle (deg)	Stresses (MPa) σ_x	σ_y	σ_z
Constrain.	Al #20	0.20	2.53	-90.00	40.08	21.58	21.58
Uniaxial	Al #21	0.22	2.11	-90.00	33.49	18.03	18.03
Tension	Al #22	0.24	2.20	-90.00	34.92	18.80	18.80
	Al #23	0.22	1.91	-90.00	30.32	16.32	16.32

Uniaxial tension and compression tests were carried out on neat specimens. The results are shown in Table 3.3

Table 3.3 Yield stress of FM73 adhesive in neat tension and neat compression.

	Adhesive thick. (mm)	Yield load (kN)	Load angle (deg)	Stress (MPa) σ_x
neat compression	7.43	19.56	90.00	-69.00
neat tension	1.86	11.91	-90.00	42.00

3.6 Failure Modes

Failure modes for various stress states are shown in the following figures.

Figure 3.5 - Failure in pure shear

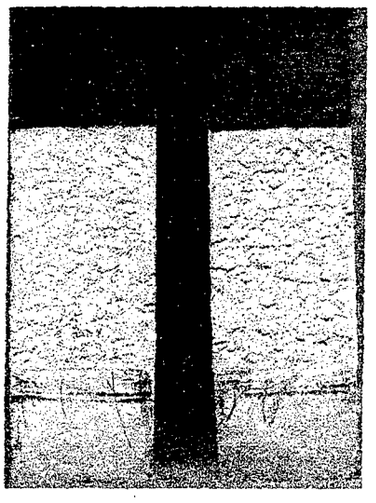

Figure 3.6 - Failure in shear-tension

(load angle of -33.23deg)

Figure 3.7 - Failure in shear-compression

(load angle of 17.19deg)

Figure 3.8 - Failure in shear-compression

(load angle of 22.92deg)

From Figures 3.5 and 3.6 it is evident that in pure shear and shear-tension cohesive failure of the adhesive occurs. Figures 3.7 and 3.8 show that under shear-compression

some adhesive failure occurs and as the load angle increases the amount of adhesive failure increases. Nevertheless, figures for specimens #12, #13, #18 and #19 shown in Appendix 3 indicate that adhesive yielding occurs before failure.

4. Evaluation of Yield Criteria

For the purpose of identifying a suitable yield criterion that can adequately describe the yielding behaviour of FM73 adhesive, the various yield criteria discussed in Section 2 will be evaluated against the experimental results. To this end, the previously described yield criteria are graphed and compared with the experimental data.

4.1 von Mises & Tresca Criteria

It is seen from equations (2.10) and (2.17) that both the Tresca and von Mises yield criteria, for the adhesive in its highly constrained state, are in the form of an ellipse with a slight difference in one of the coefficients. Both criteria are plotted with experimental results in Figure 4.1. The axes used for plotting Tresca and von Mises criteria were τ_{xy}/σ_0 and σ_x/σ_0, where σ_0 is the yield stress of the neat adhesive in tension.

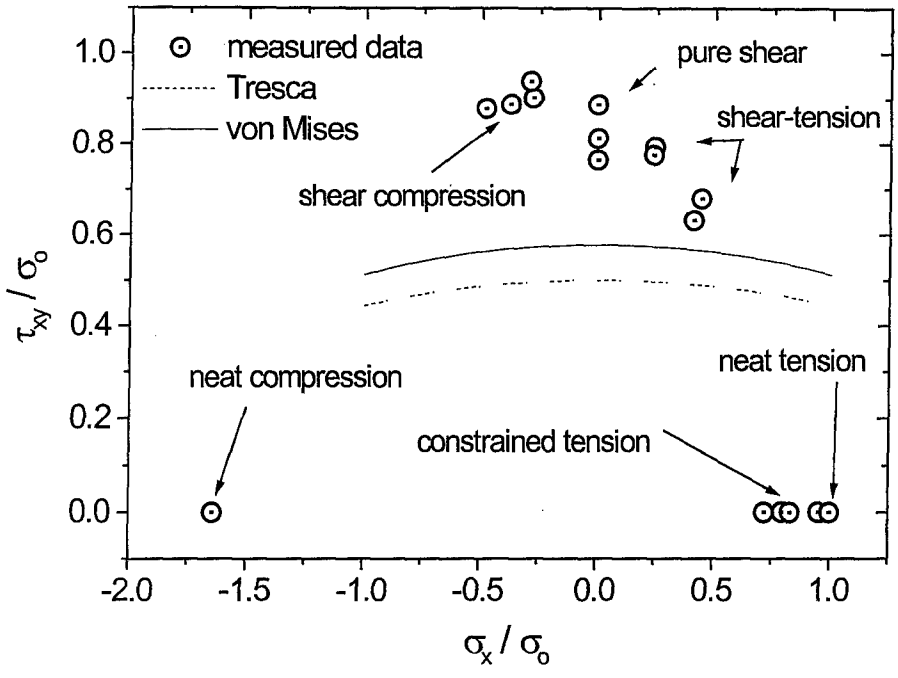

Figure 4.1. Tresca and von Mises curve fit assuming adhesive is highly constrained.

It is seen from Figure 4.1 that neither the Tresca nor the von Mises Yield criteria provide an acceptable correlation of the experimental data and therefore are inadequate for quantifying FM73 adhesive yield behaviour.

4.2 Modified von Mises and Modified Tresca Criteria

Principal stresses calculated previously were substituted in Equations (2.21), (2.22) and (2.24), giving p, τ_T and τ_M respectively. These were used to plot the experimental data in the τ vs p plane. Since the experimental data differed slightly for the two criteria due to differences between τ_T and τ_M, two separate plots were required. Figure 4.2 and 4.3 show the Modified Tresca and the Modified von Mises yield criteria curve fits.

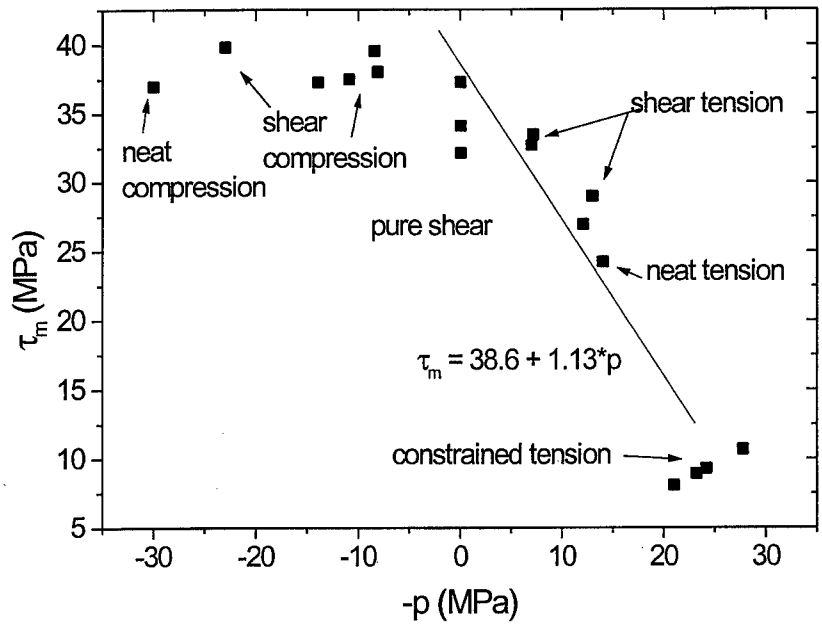

Figure 4.2. Modified Tresca Yield criterion curve fit

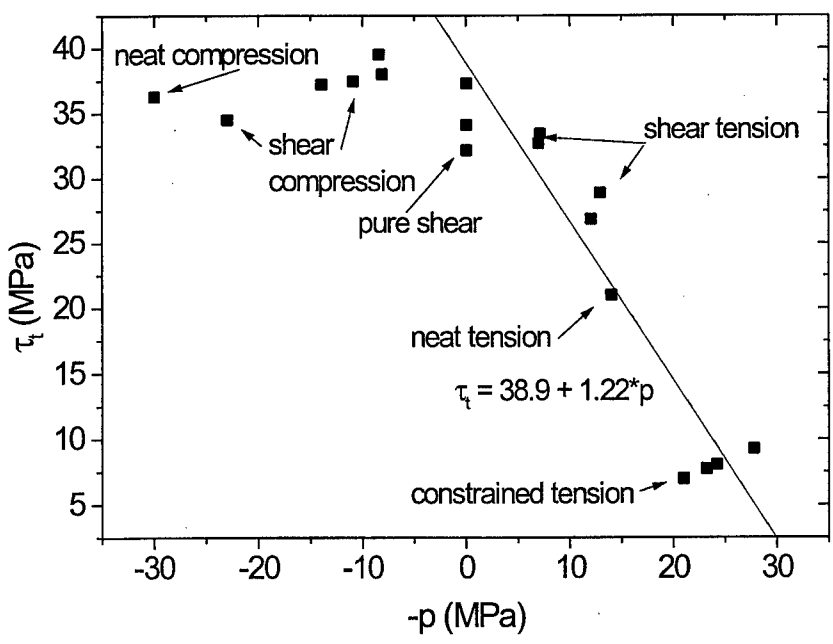

Figure 4.3. Modified von Mises Yield criterion curve fit.

It is evident that both the modified Tresca and the modified von Mises criteria can only correlate the data with positive hydrostatic stress and tend to be un-conservative when the hydrostatic stress is compressive. Therefore other yield criteria need to be examined.

4.3 Drucker-Prager and Modified Drucker-Prager/Cap Plasticity Model.

The experimental data was plotted in the τ vs p plane using Equations (2.27) and (2.28), while the theoretical curves were plotted by rearranging Equations (2.25) and (2.33) so that τ was a function of p as well as other parameters present. The results are shown in Figure 4.4. Once again, the original Drucker-Prager plasticity model can only correlate the data points corresponding to tensile hydrostatic stress. The modified Drucker-Prager/Cap Plasticity model is the only criterion that can correlate data points with both tensile and compressive hydrostatic stresses.

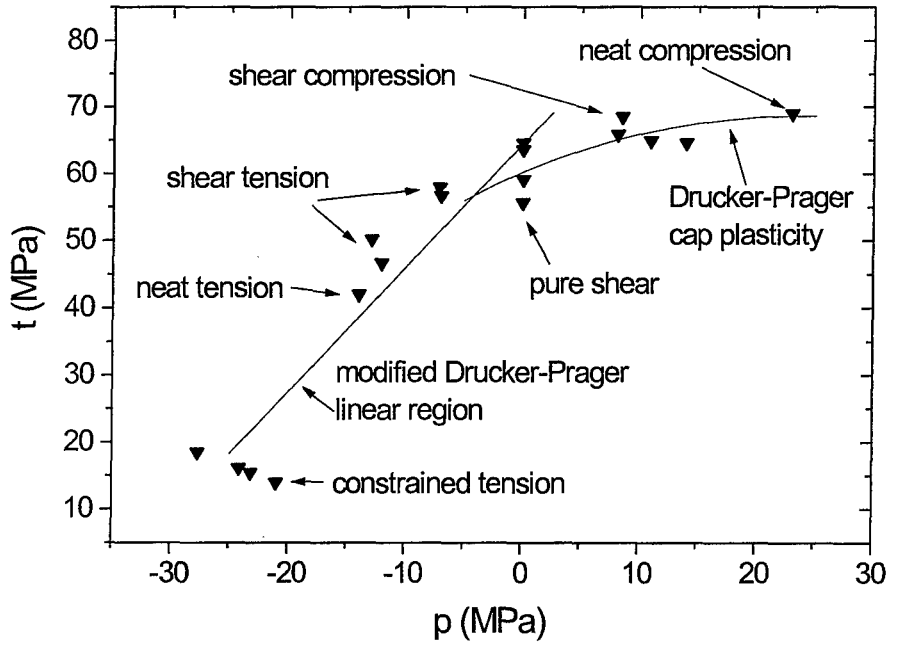

Figure 4.4. Modified Drucker-Prager curve fit.

In order to fit the modified Drucker-Prager/Cap plasticity model to the experimental results, the following parameters (Drucker-Prager variables) had to be identified:

K is the ratio of flow stress in triaxial tension to the flow stress in triaxial compression. The range of K values is limited between 0.778 and 1.0 to ensure convexity of the yield surface.

β is material angle of friction in degrees.

σ_C^0 is the yield stress in uniaxial compression.

R is cap eccentricity and controls the shape of the cap yield surface. It must be greater than 0 and is generally less than 1.

α is transition surface radius parameter. Its magnitude should be much lower than 1 and generally ranges between 0.01 and 0.05. However, a larger value of 0.191 was found in this study.

The Drucker-Prager variables listed below produced a curve which best fitted the experimental data:

K	β (deg)	σ_C^0	R	α
0.778	63.6	225.811	0.325	0.191

5. Finite Element Modelling

The main aim of finite element modelling was to validate the assumption of plane strain and to check for any stress concentrations in the specimen that may invalidate the experimental results.

5.1 Procedure

The Iosipescu model (see Figure 3.1) was developed using the pre- and post-processor Patran. Fine mesh is employed around the adhesive bond to obtain an accurate representation of the stress distribution in that region. The mesh is shown in Figure 5.1.

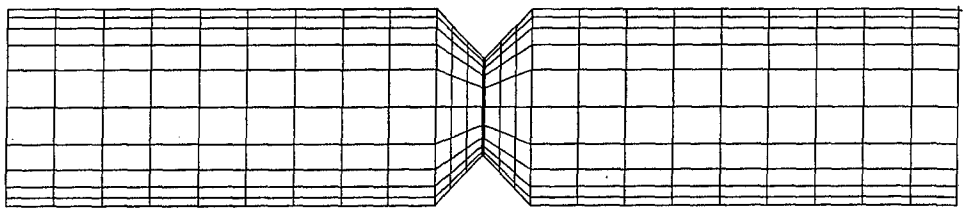

Figure 5.1. The Iosipescu specimen finite element mesh.

The material properties given below were then assigned to adherent and adhesive regions and the load and boundary conditions were applied. The properties chosen included the Drucker-Prager variables, as listed in Section 4, and allowed both elastic and plastic behaviour of the adhesive bond to be modelled.

Aluminium alloy	E=72000MPa	ν=0.33
FM73 adhesive	E=2160MPa	ν=0.35

The load and boundary conditions were also an important part of the analysis because of the stress distribution dependence on these parameters. These were based on the pure shear load case as described in Broughton's Phd thesis [4]. The following load and boundary conditions were therefore applied to the model:

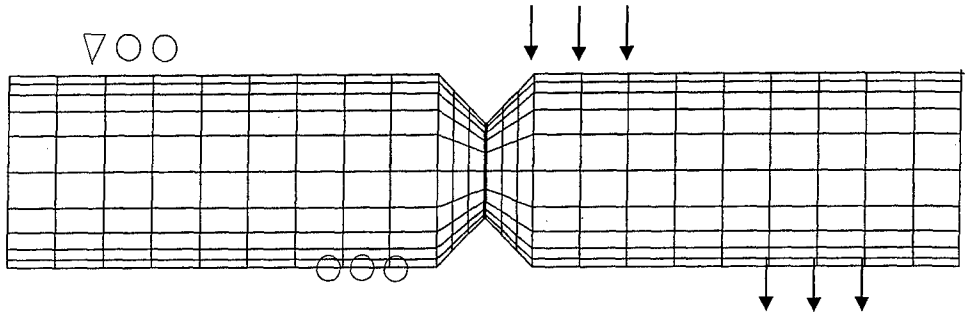

Figure 5.2. Load and boundary conditions (pure shear).

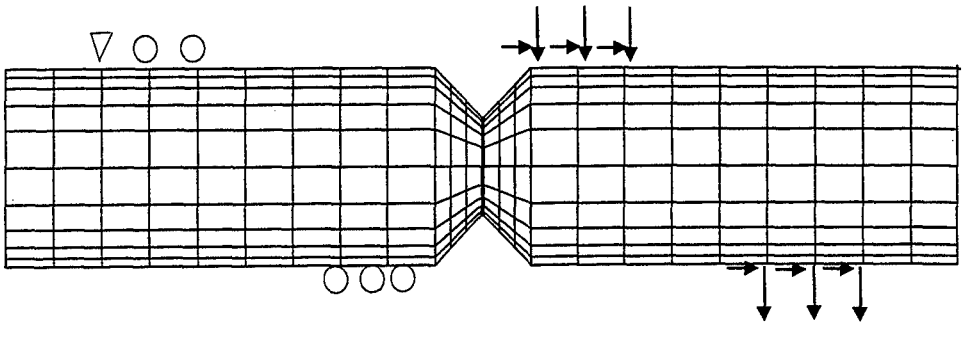

Figure 5.3. Load and boundary conditions (combined shear-tension).

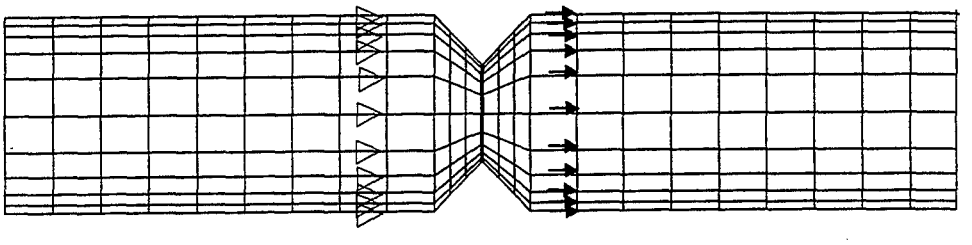

Figure 5.4 Load and boundary conditions (constrained uniaxial tension).

5.2 Results

The Iosipescu specimen was originally designed to apply pure shear and Figure 5.5 shows the normalised shear stress distribution across the width of the adhesive layer at its midplane.

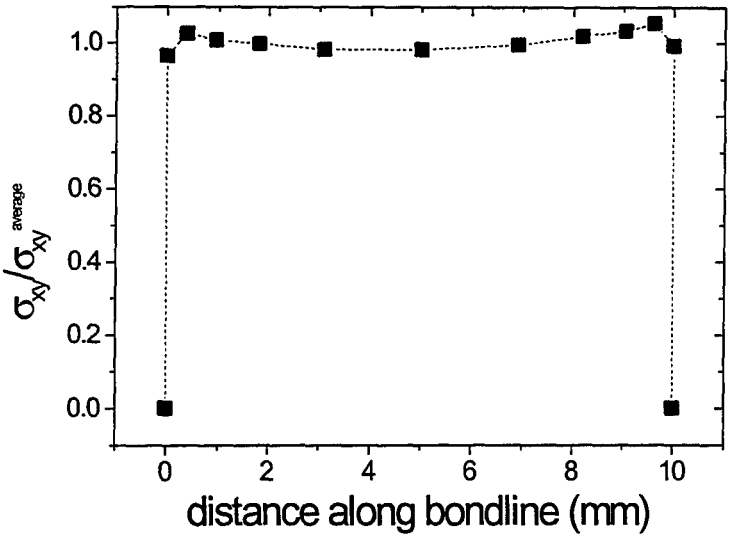

Figure 5.5. Shear stress distribution in the Iosipescu specimen.

Figure 5.5 shows a reasonably uniform distribution of shear stress in the adhesive.

The validity of Equation (2.9), which relates to the assumption of the adhesive being highly constrained, was examined using 3D ABAQUS FE model results. Equation (2.9) dictates that the plot of normalised stresses σ_y/σ_x and σ_z/σ_x against the adhesive length (along line through the middle of adhesive), should approach $\nu/(1-\nu)$ or 0.538 for adhesive with ν=0.35. The FE results for uniaxial tension applied to a modified Iosipescu specimen are shown in Figure 5.6 (stresses are normalised against tensile stress, σ_x).

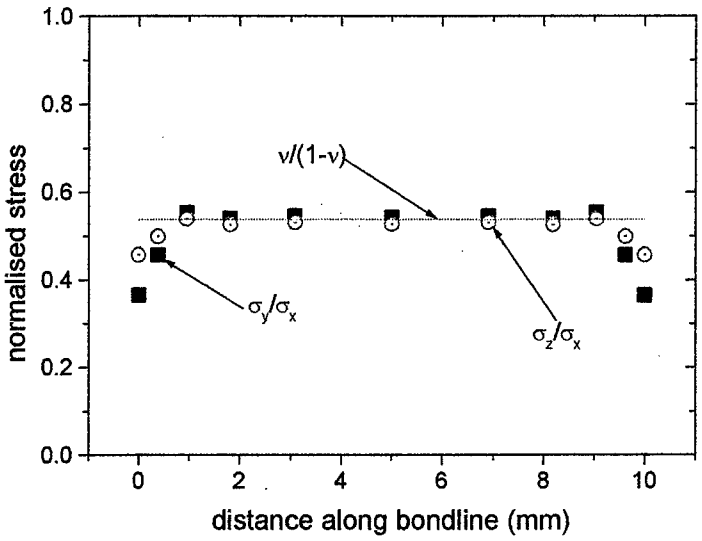

Figure 5.6. Normalised stresses along bondline (constrained uniaxial tension) – 3D model.

Figures 5.6 shows that the plane strain assumption is generally valid across the adhesive length as the normalised stresses approach a theoretical value of 0.538. These results from 3D models validate the use of 2D plane strain models to investigate the stresses in the adhesive. The highly constrained nature of the adhesive and the approach taken in the experimental section is also validated by these results.

The following figures are taken from results from 2D FE models. Around the edges it is observed that the normalised stresses deviate significantly from their expected values. This is due to the edge effects in butt-type joints that cause stress concentrations. To confirm this behaviour, stresses in each direction were plotted against the adhesive length as shown in Figures 5.7 and 5.8. These were normalised with respect to the average tensile stress, σ_{xav} obtained from the reaction forces at the FE model constraints.

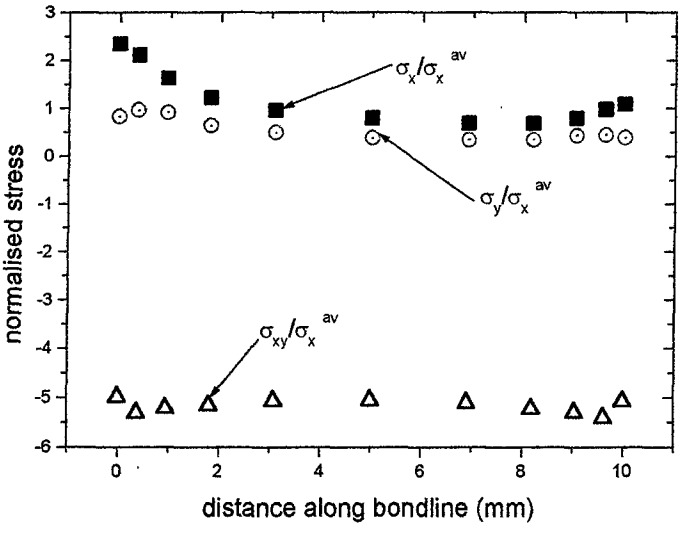

Figure 5.7. Stresses along bondline (combined shear-tension) – 2D model.

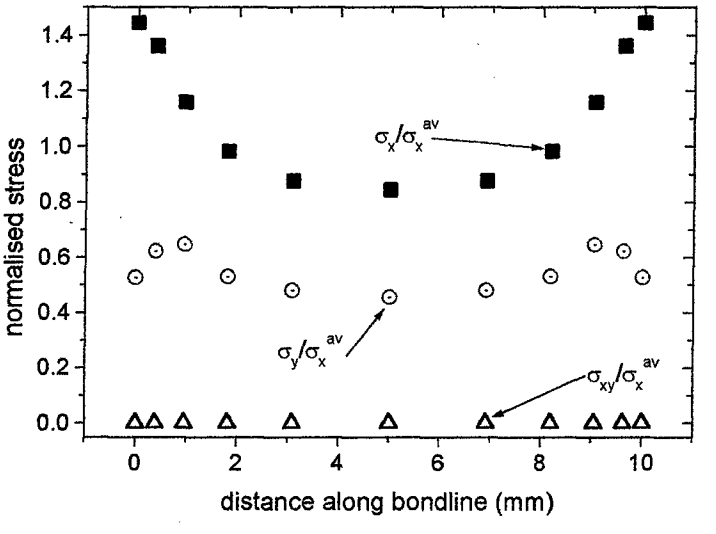

Figure 5.8. Stresses along bondline (constrained uniaxial tension) – 2D model.

From Figures 5.7 and 5.8, it is clearly seen that stresses at the adhesive edges are larger than those towards the middle, thus showing that the edge effects are present as stated earlier. However, stress concentrations are mostly limited to the specimen edges, with

the bulk of the adhesive being close to the average stress as assumed in the experimental results section. Therefore the adhesive yield results are expected to be correct to a first approximation.

6. Conclusions

From the present study into the plastic yielding behaviour of FM73 adhesive under combined stress states, the following conclusions may drawn:

- The adhesive is in a highly constrained state as indicated by the finite element results
- The plane strain assumption is valid for the majority of the bond line, as verified by finite element analysis.
- The adhesive is pressure sensitive, but this sensitivity is truncated at zero hydrostatic stress and at compressive hydrostatic stress the adhesive becomes pressure insensitive.
- The Modified Drucker-Prager/Cap Plasticity model provides the best yield function for modelling adhesive behaviour.

7. References

1. Bartholomeusz, R. A., Searl, A., Baker, A. A. and Chester, R. J., *Bonded Composite Reinforcement of the F/A-18 Y470.5 Bulkhead, Applications with Through-Thickness Stresses,* International Aerospace Congress, Sydney, 24-27 Feb 1997.

2. Baker, A. A., *Crack patching experimental studies, practical applications,* Chapter 6 in *Bonded Repair of Aircraft Structures,* Ed. By Baker, A. A. and Jones, R., Martinus Nijhoff Publishers, Dordrecht, 1988.

3. Haward, R. N. (1973). *The Physics of Glassy Polymers,* Applied Science Publishers Pty. Ltd., London.

4. Broughton, W. R. (1989). *Shear Properties of Unidirectional Carbon Fibre Composites.* Darwin College, Cambridge.

5. Wycherley, G. W., Mestan, S. A. and Grabovac, I., *A Method for Uniform Shear Stress-Strain Analysis of Adhesives,* ASTM JOTE May 1990.

6. Dieter, G. E. (1986). *Mechanical Metallurgy,* Third Edition. McGraw-Hill Inc., U.S.A.

7. Bowden, P. B. and Jukes, J. A., *The Plastic Flow of Isotropic Polymers,* J. of Materials Science 7 (1972) 52-63.

8. ABAQUS (1995). *Theory Manual,* Version 5.5. Hibbitt, Karlsson & Sorensen Inc., U.S.A.

9. ABAQUS (1996). *Standard User's Manual,* Volume 1, Version 5.6. Hibbitt, Karlsson & Sorensen Inc., U.S.A.

10. ABAQUS (1996). *Standard User's Manual,* Volume 3, Version 5.6. Hibbitt, Karlsson & Sorensen Inc., U.S.A.

11. Chiang, M. Y. M. and Chai, H. (1994). *Plastic Deformation Analysis of Cracked Adhesive Bonds Loaded in Shear.* Int. J. Solids Struct. 31, 2477-2490.

12. Woolgar, B. F. (1993?) *The Application of the Iosipescu Shear Test to Structural Adhesives.* Final Year Thesis, Mechanical Engineering Department, Queensland University of Technology, Brisbane.

13. Ignjatovic, M., *Yield Behaviour of Structural Adhesives in Bonded Joints,* Vacation Scholar Thesis, AMRL, 1998.

Appendices

Appendix 1 - State of Stress in Three Dimensions

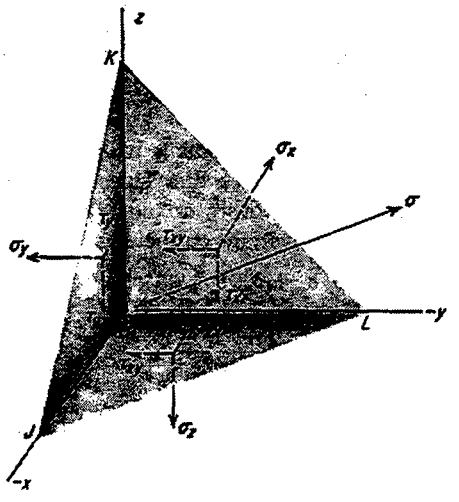

Figure A.1 - Stresses acting on elemental free body

The equilibrium of forces in x, y and z directions from Figure A.1 leads to the following set of homogenous linear equations

$$(\sigma - \sigma_x)l - \tau_{yx}m - \tau_{zx}n = 0 \quad \text{(A.1)}$$

$$-\tau_{xy}l + (\sigma - \sigma_y)m - \tau_{zy}n = 0 \quad \text{(A.2)}$$

$$-\tau_{xz}l - \tau_{yz}m + (\sigma - \sigma_z)n = 0 \quad \text{(A.3)}$$

Here, l,m and n are the direction cosines of σ.

In order to find a non-trivial solution, the determinant of the l, m and n coefficients must be equal to zero

$$\begin{vmatrix} \sigma-\sigma_x & -\tau_{yx} & -\tau_{zx} \\ -\tau_{xy} & \sigma-\sigma_y & -\tau_{zy} \\ -\tau_{xz} & -\tau_{yz} & \sigma-\sigma_z \end{vmatrix} = 0$$

$$\Rightarrow \sigma^3 - (\sigma_x+\sigma_y+\sigma_z)\sigma^2 + (\sigma_x\sigma_y+\sigma_y\sigma_z+\sigma_x\sigma_z-\tau_{xy}^{\ 2}-\tau_{yz}^{\ 2}-\tau_{xz}^{\ 2})\sigma - (\sigma_x\sigma_y\sigma_z+2\tau_{xy}\tau_{yz}\tau_{xz}-\sigma_x\tau_{yz}^{\ 2}-\sigma_y\tau_{xz}^{\ 2}-\sigma_z\tau_{xy}^{\ 2}) = 0 \quad \text{(A.4)}$$

The above cubic equation has three roots (σ_1, σ_2 and σ_3) known as the principal stresses. Since $\tau_{xz} = \tau_{yz} = 0$, Equation (A.4) simplifies to

$$\sigma^3 - (\sigma_x+\sigma_y+\sigma_z)\sigma^2 + (\sigma_x\sigma_y+\sigma_y\sigma_z+\sigma_x\sigma_z-\tau_{xy}^{\ 2})\sigma - (\sigma_x\sigma_y\sigma_z-\sigma_z\tau_{xy}^{\ 2}) = 0 \quad \text{(A.5)}$$

and from Equation (A.3), it was found that one of the three principal stresses is

$$\sigma_i = \sigma_z \quad \text{(A.6)}$$

Dividing Equation (A.5) by Equation (A.6) leads to the following quadratic equation

$$\sigma^2 - (\sigma_x+\sigma_y)\sigma + (\sigma_x\sigma_y-\tau_{xy}^{\ 2}) \quad \text{(A.7)}$$

Therefore the other two principal stresses are found by solving Equation (A.7)

$$\sigma_i = \frac{(\sigma_x+\sigma_y) \pm \sqrt{(\sigma_x+\sigma_y)^2 - 4(\sigma_x\sigma_y-\tau_{xy}^{\ 2})}}{2} \quad \text{(A.8)}$$

i=1 or 2 or 3 in Equations (A.6) and (A.8) depending on the relative magnitudes of the principal stresses. i=1 for the maximum principal stress and i=3 for the minimum principal stress.

Appendix 2 - Force-Displacement Graphs

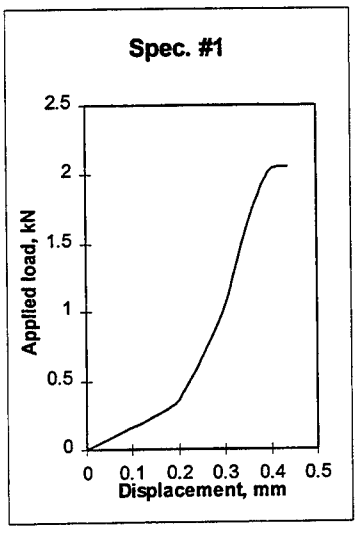

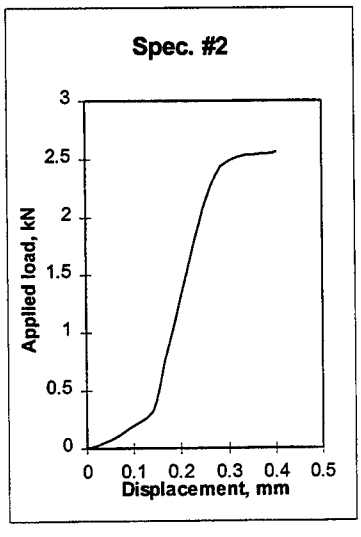

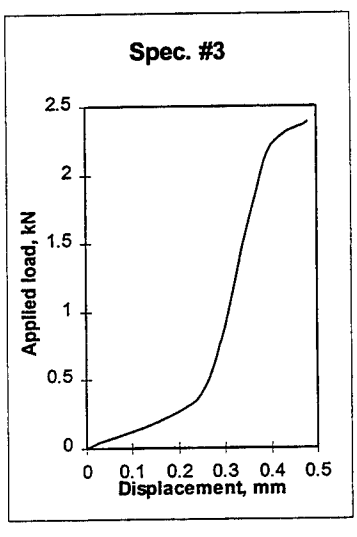

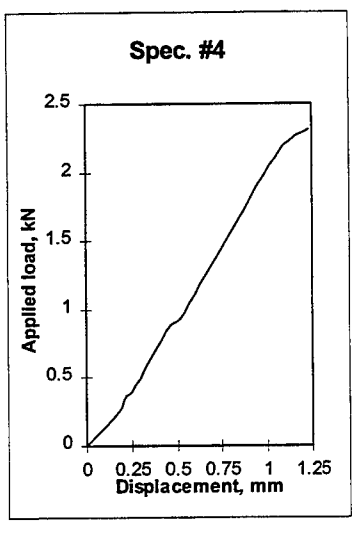

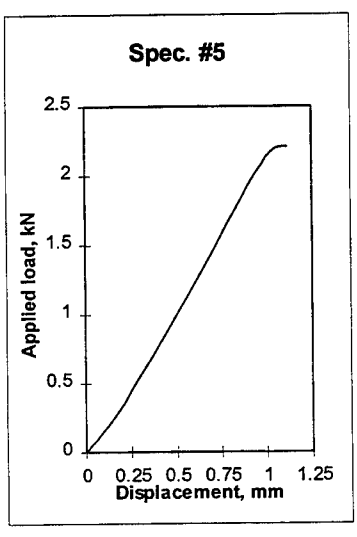

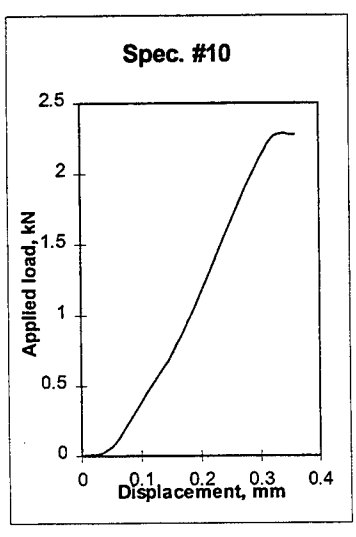

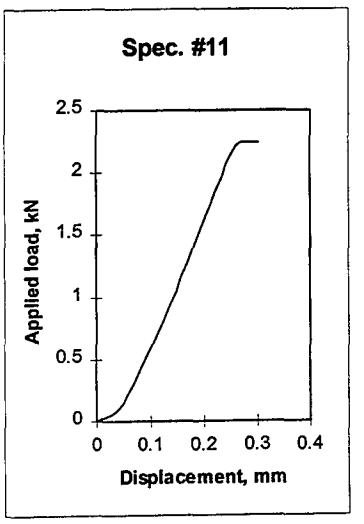
Spec. #11
Applied load, kN
2.5
2
1.5
1
0.5
0
0 0.1 0.2 0.3 0.4
Displacement, mm

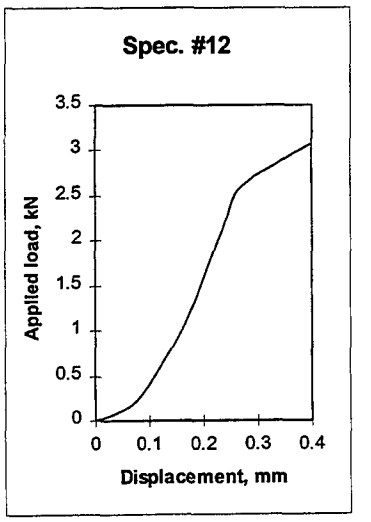
Spec. #12
Applied load, kN
3.5
3
2.5
2
1.5
1
0.5
0
0 0.1 0.2 0.3 0.4
Displacement, mm

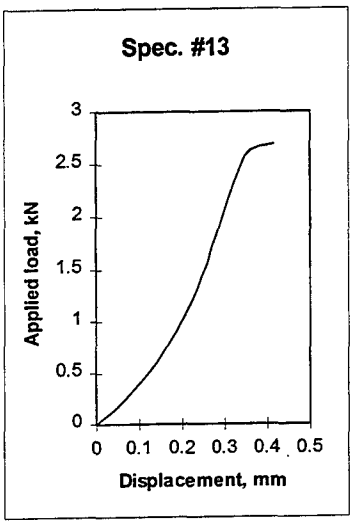
Spec. #13
Applied load, kN
3
2.5
2
1.5
1
0.5
0
0 0.1 0.2 0.3 0.4 0.5
Displacement, mm

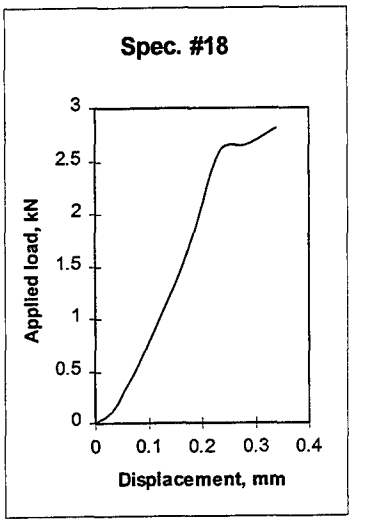
Spec. #18
Applied load, kN
3
2.5
2
1.5
1
0.5
0
0 0.1 0.2 0.3 0.4
Displacement, mm

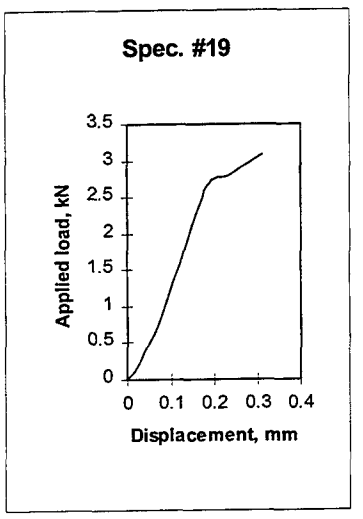
Spec. #19
Applied load, kN
3.5
3
2.5
2
1.5
1
0.5
0
0 0.1 0.2 0.3 0.4
Displacement, mm

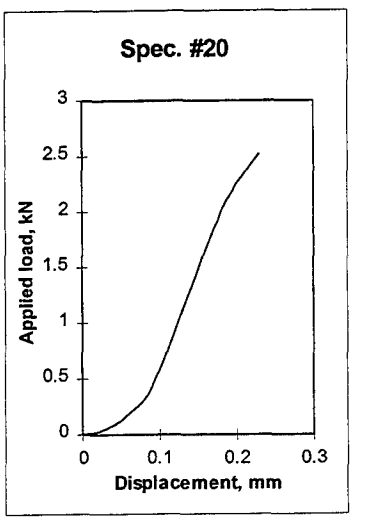
Spec. #20
Applied load, kN
3
2.5
2
1.5
1
0.5
0
0 0.1 0.2 0.3
Displacement, mm

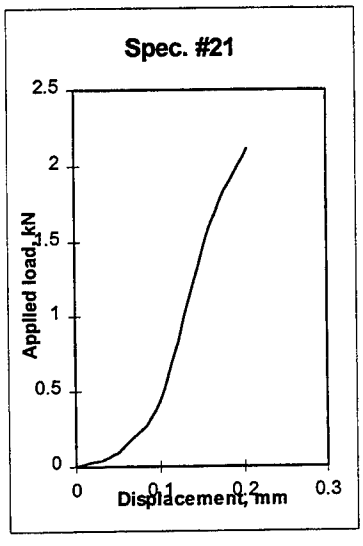
Spec. #21
Applied load, kN
2.5
2
1.5
1
0.5
0
0
0.1
0.2
0.3
Displacement, mm

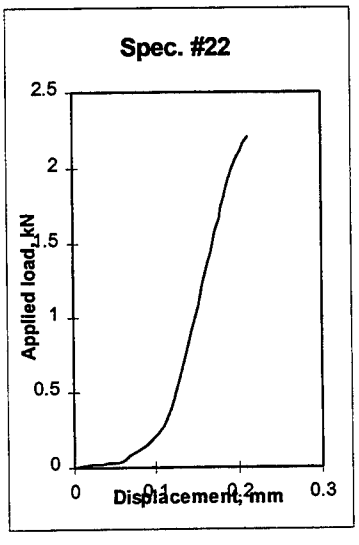
Spec. #22
Applied load, kN
2.5
2
1.5
1
0.5
0
0
0.1
0.2
0.3
Displacement, mm

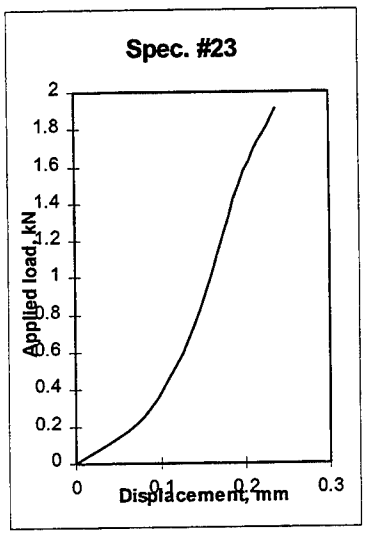
Spec. #23
Applied load, kN
2
1.8
1.6
1.4
1.2
1
0.8
0.6
0.4
0.2
0
0
0.1
0.2
0.3
Displacement, mm

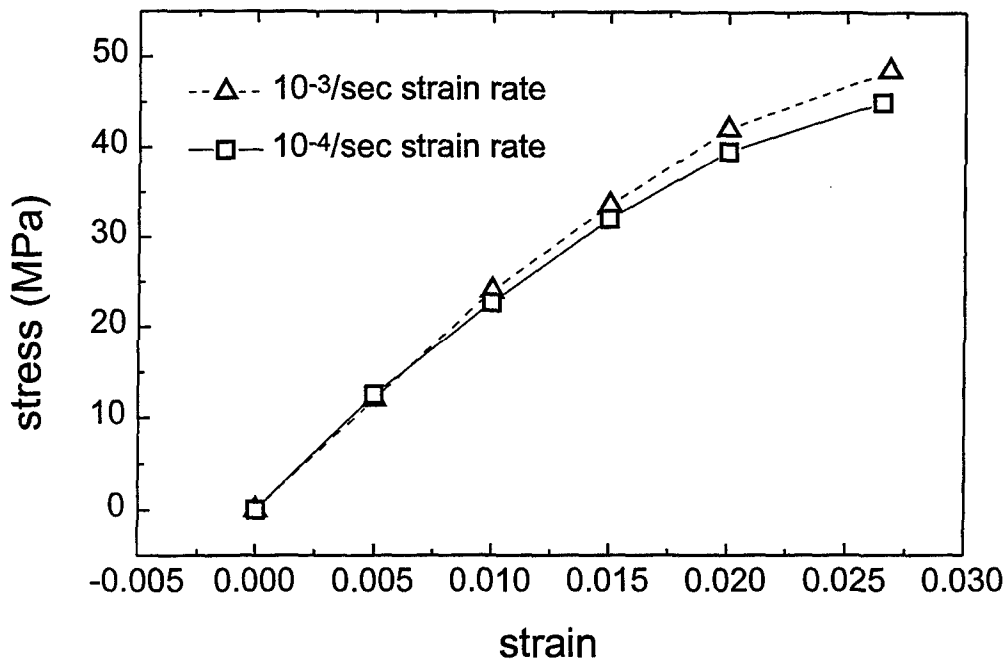

Tensile Tests on Neat FM73 Adhesive.

DISTRIBUTION LIST

The Yield Behaviour of a Structural Adhesive under Complex Loading

Mladen Ignjatovic, Peter Chalkley and Chun Wang

AUSTRALIA

DEFENCE ORGANISATION

Task Sponsor
RAAF ASI - 1A

S&T Program
Chief Defence Scientist
FAS Science Policy } shared copy
AS Science Corporate Management
Director General Science Policy Development
Counsellor Defence Science, London (Doc Data Sheet)
Counsellor Defence Science, Washington (Doc Data Sheet)
Scientific Adviser to MRDC Thailand (Doc Data Sheet)
Director General Scientific Advisers and Trials/Scientific Adviser Policy and Command (shared copy)
Navy Scientific Adviser (Doc Data Sheet and distribution list only)
Scientific Adviser - Army (Doc Data Sheet and distribution list only)
Air Force Scientific Adviser
Director Trials

Aeronautical and Maritime Research Laboratory
Director

Chief of Airframes and Engines Division
RLFM, RLACS
Richard Chester – Functional Head Composites
Author(s): Peter Chalkley and Francis Rose (1 copy each)

DSTO Library
Library Fishermens Bend
Library Maribyrnong
Library Salisbury (2 copies)
Australian Archives
Library, MOD, Pyrmont (Doc Data sheet only)

Capability Development Division
Director General Maritime Development (Doc Data Sheet only
Director General Land Development (Doc Data Sheet only
Director General C3I Development (Doc Data Sheet only)

Army
ABCA Office, G-1-34, Russell Offices, Canberra (4 copies)
SO (Science), DJFHQ(L), MILPO Enoggera, Queensland 4051 (Doc Data Sheet only)
NAPOC QWG Engineer NBCD c/- DENGRS-A, HQ Engineer Centre Liverpool Military Area, NSW 2174 (Doc Data Sheet only

Air Force
ASI-SRS Max Davis

Intelligence Program
DGSTA Defence Intelligence Organisation

Corporate Support Program (libraries)
OIC TRS, Defence Regional Library, Canberra
Officer in Charge, Document Exchange Centre (DEC) (Doc Data Sheet and distribution list only)
*US Defence Technical Information Center, 2 copies
*UK Defence Research Information Centre, 2 copies
*Canada Defence Scientific Information Service, 1 copy
*NZ Defence Information Centre, 1 copy
National Library of Australia, 1 copy

UNIVERSITIES AND COLLEGES
Australian Defence Force Academy
Library
Head of Aerospace and Mechanical Engineering
Deakin University, Serials Section (M list), Deakin University Library, Geelong, 3217
Senior Librarian, Hargrave Library, Monash University
Librarian, Flinders University

OTHER ORGANISATIONS
NASA (Canberra)
AGPS

OUTSIDE AUSTRALIA

ABSTRACTING AND INFORMATION ORGANISATIONS
INSPEC: Acquisitions Section Institution of Electrical Engineers
Library, Chemical Abstracts Reference Service
Engineering Societies Library, US
Materials Information, Cambridge Scientific Abstracts, US
Documents Librarian, The Center for Research Libraries, US

INFORMATION EXCHANGE AGREEMENT PARTNERS
Acquisitions Unit, Science Reference and Information Service, UK
Library - Exchange Desk, National Institute of Standards and Technology, US
National Aerospace Laboratory, Japan
National Aerospace Laboratory, Netherlands

SPARES (10 copies)

Total number of copies: **59**

DEFENCE SCIENCE AND TECHNOLOGY ORGANISATION
DOCUMENT CONTROL DATA

1. PRIVACY MARKING/CAVEAT (OF DOCUMENT)

2. TITLE

The Yield Behaviour of a Structural Adhesive under Complex Loading

3. SECURITY CLASSIFICATION (FOR UNCLASSIFIED REPORTS THAT ARE LIMITED RELEASE USE (L) NEXT TO DOCUMENT CLASSIFICATION)

Document	(U)
Title	(U)
Abstract	(U)

4. AUTHOR(S)

Mladen Ignjatovic, Peter Chalkley and Chun Wang

5. CORPORATE AUTHOR

Aeronautical and Maritime Research Laboratory
PO Box 4331
Melbourne Vic 3001 Australia

6a. DSTO NUMBER	6b. AR NUMBER	6c. TYPE OF REPORT	7. DOCUMENT DATE
DSTO-TR-0728	AR-010-646	Technical Report	September 1998

8. FILE NUMBER	9. TASK NUMBER	10. TASK SPONSOR	11. NO. OF PAGES	12. NO. OF REFERENCES
M1/9/563	98/188	RAAF-ASI-IA	33	13

13. DOWNGRADING/DELIMITING INSTRUCTIONS

14. RELEASE AUTHORITY

Chief, Airframes and Engines Division

15. SECONDARY RELEASE STATEMENT OF THIS DOCUMENT

Approved for public release

OVERSEAS ENQUIRIES OUTSIDE STATED LIMITATIONS SHOULD BE REFERRED THROUGH DOCUMENT EXCHANGE CENTRE, DIS NETWORK OFFICE, DEPT OF DEFENCE, CAMPBELL PARK OFFICES, CANBERRA ACT 2600

16. DELIBERATE ANNOUNCEMENT

No Limitations

17. CASUAL ANNOUNCEMENT Yes

18. DEFTEST DESCRIPTORS

Bonded composite repairs, aircraft structures

19. ABSTRACT

Recent developments in bonded composite repair technology at the Aeronautical and Maritime Research Laboratory (AMRL) have been in the area of repairs to curved surfaces, eg. the proposed repairs to the F/A-18 aileron hinge and the F/A-18 bulkhead crotch region. Bonded composite repairs to curved surfaces induce through-thickness stresses as well as shear stresses in the adhesive. The yield behaviour of AMRLs most common repair adhesive - FM73 - has not been investigated under such conditions of combined loading.

Reported herein is a yield function for the repair adhesive FM73, based upon the Modified Drucker-Prager/Cap Plasticity model. This yield function was selected based on experiments on a test specimen subjected to a range of combined stress states. A finite element (FE) analysis of test specimen (Iosipescu test specimen modified for adhesives) was carried out to establish its validity for obtaining data.

A set of constants was obtained for the Modified Drucker-Prager/Cap Plasticity model of FM73 adhesive that enables detailed FE analyses of bonded repairs to curved surfaces.